WILEY ONLINE LIBRARY EarlyView publication on wileyonlinelibrary.com
(issue and page numbers not yet assigned;
citable using Digital Object Identifier – **DOI**)

Phys. Status Solidi A, 1–4 (2013) / **DOI** 10.1002/pssa.201228734

physica status solidi a
www.pss-a.com
applications and materials science

Proton irradiation effects on thermal transport in individual single-crystalline Bi nanowires

Jong Wook Roh[1,2,†], Dai Ho Ko[3,†], Joohoon Kang[1], Min Kyung Lee[1], Joo Hee Lee[3], Cheol Woo Lee[4], Kyu Hyoung Lee[2], Jin-Seo Noh[,5], and Wooyoung Lee[*,1]**

[1] Department of Materials Science and Engineering, Yonsei University, 262 Seongsanno, Seoul 120-749, Korea
[2] Advanced Materials Research Center, Samsung Advanced Institute of Technology, Samsung Electronics, Gyeonggi 446-712, Korea
[3] Korea Aerospace Research Institute, Daejeon 305-333, Korea
[4] Korea Atomic Energy Research Institute, Daejeon 305-353, Korea
[5] Department of Nano-Physics, Gachon University, 1342 Seongnamdaero, Seongnam-si, Gyeonggi-do, Korea

Received 30 October 2012, revised 24 February 2013, accepted 5 March 2013
Published online 15 April 2013

Keywords bismuth, MEMS, nanowires, proton irradiation, thermal conductivity

[*] Corresponding author: e-mail wooyoung@yonsei.ac.kr, Phone: +82 2 2123 2834, Fax: +82 2 312 5375
[**] e-mail jinseonoh@gachon.ac.kr, Phone: +82 2 2123 7802, Fax: +82 2 312 5375
[†] These authors contributed equally to this work.

We investigated the proton irradiation effect of thermal conductivities for individual single-crystalline Bi nanowires grown by the on-film formation of nanowires (ON–OFF). The thermal conductivities of Bi nanowires with diameter of 154 and 112 nm were measured using suspended devices before and after proton irradiation, respectively. It was founded thermal conductivities of Bi nanowires appreciably decrease after proton irradiation, which was caused by the destruction of single-crystallinity due to the high-energy proton impingement. This result indicates the defects of Bi nanowires created by proton drastically limit the mean free paths of phonons, resulting in the change of thermal transport of Bi nanowires.

1 Introduction With a development of nanotechnology, the researches on synthesis and characteristics of low dimensional nanostructure have been challenging issues of scientific and technological concern. In particular, single-crystalline bismuth (Bi) nanowires has attracted great attention due to its unique transport properties such as long mean free path, high mobility [1], and large magnetoresistance [2]. Furthermore, ever since Dresselhaus et al. [3, 4] predicted theoretically that thermoelectric property of single crystalline Bi nanowires would increase by quantum confinement effect and size effect, the study on the transport phenomena of Bi nanowires has been intensively researched [5–7]. Most of experimental studies on Bi nanowires so far have focused on the unique electrical properties of Bi nanowires [8–13]. Although theoretical studies on the phonon transport in nanowires have revealed the thermal transport was effectively controlled by nanostructure [14–16], only a few studies have been carried out on thermal transport in Bi nanowires due to the difficulties of measuring properties of individual nanowires. Moore et al. [17] have reported thermal conductivity (κ) suppression in Bi nanowires due to enhanced boundary phonon scattering. In prior report, we have found that the highly anisotropic thermal transport properties in single crystalline Bi nanowires were caused by unique crystal structure of Bi [18]. Although electrical and thermal transport properties are known to be sensitive to radiation-induced defects in bulk [19, 20], even so, there has been no systematic study on the proton irradiation effect of thermal conductivities for individual single-crystalline Bi nanowires, which is of significant importance in predicting the thermal transport phenomena in nanostructure. In this report, we investigated the proton irradiation effects on the thermal conductivity and crystal structure of individual single-crystalline Bi nanowires grown by the on-film formation of nanowires (ON–OFF).

2 Experiment Single-crystalline Bi nanowires were grown using the OFF–ON [1, 21], which is a stress-activated nanowire growth method. As shown in Fig. 1a, the Bi nanowires grown by this method were uniform in diameter

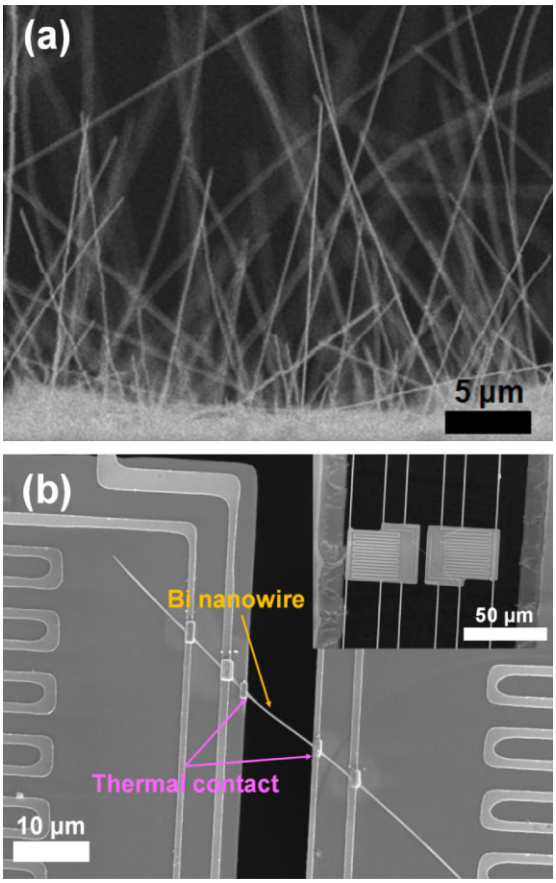

Figure 1 (a) Field emission scanning electron microscopy (FE-SEM) image of single-crystalline Bi nanowires grown by the OFF–ON method. (b) SEM image of an individual Bi nanowire placed on the suspended MEMS. The membranes were thermally isolated and supported with six legs (inset).

with aspect ratios exceeding 1000. To measure the thermal conductivities of the Bi nanowires, they were dispersed on suspended MEMS by a drop-casting method. The suspended MEMS, which consist of two adjacent silicon nitride (SiN_x) membranes and six long beams as shown in the inset of Fig. 1b, were employed for measuring thermal conduction only through individual nanowires without thermal conduction through the substrate. The detail procedure of thermal conductivity measurement was introduced in prior report [22–24]. A Pt resistance thermometer (PRT) coil on each membranes act as both a heater to increase the temperature of a membrane and a thermometer to measure the temperature of the membrane. In order to reduce the thermal contact resistance between the Bi nanowires and each membrane, Pt/C thermal contacts were locally deposited using a dual-beam focused ion beam (FIB), as shown in Fig. 1b. The temperature difference between heating and sensing membranes was optimized within 5 K to prevent heat conduction by radiation. The thermal conductivity measurement was carried out in a cryostat with a vacuum of less than 1×10^{-6} Torr to eliminate convectional heat loss. Typical temperature scan range was 40–300 K. In this study, two diameters (112 and 154 nm) of nanowires were under focus. Proton irradiation experiment was conducted using cyclotron facility in the Korea Atomic Energy Research Institute (KAERI). The irradiation beam energy, affluence, and total dose were 17.2 MeV, 5×10^{12} cm^{-2}, and 2 Mrad (Si), respectively. The total number of protons that irradiated the Bi nanowires was calculated to be 46,000 and 61,600 for the respective 112 and 154 nm nanowires.

3 Results and discussion The thermal conductivities of Bi nanowires with two different diameters were measured before proton irradiation and the results are shown in Fig. 2a (upper two curves). The thermal conductivities of 112 nm nanowire are lower than those of 154 nm nanowire over the entire temperature range and they are 2.00 W/m · K (112 nm) and 2.93 W/m · K (154 nm), respectively, at

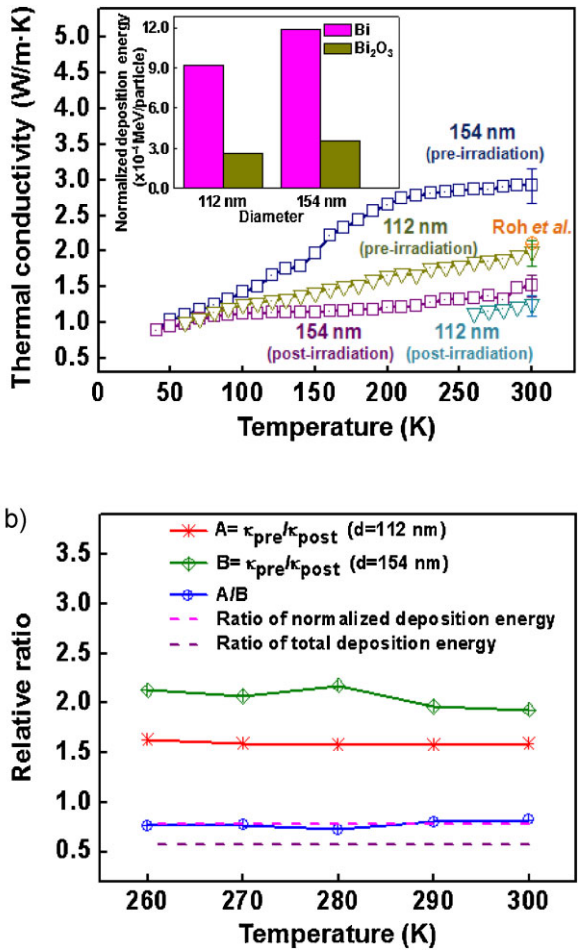

Figure 2 (a) The thermal conductivities of individual Bi nanowires with $d = 112$ and 154 nm before and after proton irradiation. The inset shows the normalized deposition energy onto the Bi nanowires with the respective diameters. (b) The ratio of thermal conductivities before and after proton irradiation for Bi nanowires with $d = 112$ nm (A) and 154 nm (B) over the range of 260–300 K. The ratios of normalized deposition energy and total deposition energy are compared with the A/B.

300 K. The measured values are coincident with those of Bi nanowires with [110] growth direction from our previous work [18], showing the size-dependence of thermal conductivity. After measuring thermal conductivity, the proton irradiation experiment was performed on the same Bi nanowires which were stuck to the suspended MEMS and the samples were located at the center of the proton beam to minimize a dependency of energy and flux on the position. The thermal conductivities after proton irradiation are also displayed in Fig. 2a (bottom two curves). For both diameters, the thermal conductivities of the proton-irradiated Bi nanowires are significantly lower than the values before irradiation. Specifically, the post-irradiation thermal conductivities at 300 K are 1.26 and 1.51 W/m · K for the respective 112 and 154 nm nanowires, corresponding to a thermal conductivity change ratio $(=(\kappa_{\text{pre-irradiation}} - \kappa_{\text{post-irradiation}})/\kappa_{\text{pre-irradiation}} \times 100)$ of about 37 and 48% for each diameter. As a comparison, the resistance of the Pt coils of the suspended membrane was measured to be 3.492 and 3.521 kΩ before and after proton irradiation, indicating the suspended MEMS itself was not seriously damaged by exposure to protons. These results suggest that the thermal transport in Bi nanowires was suppressed by some scattering sources such as point defects and dislocations generated by proton-irradiation [19, 20].

In order to correlate the change of thermal conductivity with the magnitude of proton irradiation, the irradiation energy on Bi layer was calculated by linear energy transfer (LET, or dE/dx), which explains the energy loss per unit distance. When a proton penetrates materials, it interacts with the target atoms and loses its energy in various ways including elastic scattering and inelastic scattering. The energy loss can be expressed by the Bethe formula as follows [25]:

$$-\frac{\mathrm{d}E}{\mathrm{d}x} = \frac{4\pi e^4 z^2}{m_0 v^2} NZ \left[\ln \frac{2m_0 v^2}{I} - \ln \left[1 - \frac{v^2}{c^2} \right] - \frac{v^2}{c^2} \right], \qquad (1)$$

where v is the particle velocity, z particle energy, N electron density, Z atomic number of the absorber atom, m_0 electron rest mass, e electron charge, I average excitation, and ionization potential of the absorber. Since the paths of the protons in the material are not usually straight but rather scatter when they encounter target atoms, we adopted a Monte-Carlo radiation transport tool, which was named Monte-Carlo N-Particle Transport Code System (MCNPX) version 2.4.0 [26]. In order to simulate the irradiation experiments using the MCNPX, we assumed that the Bi nanowires were irradiated by the uniform monochromatic beam since the beam profile could be regarded as a constant within the dimension of the Bi nanowires. Therefore, we calculated the energy deposition assuming that surface-proton sources are collimated with a single energy of 17.3 MeV. Geometry of the nanowires was simplified as a cylinder of Bi core with a bismuth oxide (Bi_2O_3) shell. For the statistical reliability, the particles of 2×10^9 were calculated. Under these conditions, calculated total deposition energies were 42.297 and 73.242 MeV, respectively, for 112 and 154 nm nanowires. As shown in the inset of Fig. 2a, the normalized deposition energies, which are total deposition energies divided by the numbers of incident particles, are 9.1951×10^{-4} and 1.189×10^{-3} MeV/particle for the respective 112 and 154 nm nanowires. From this result, it is found that normalized deposition energy is larger for thicker nanowires, explaining that more defects may be induced into the thicker nanowires from proton irradiation [19, 20], which greatly reduce their thermal conductivities. When the effect of proton irradiation is defined as the relative ratio of $\kappa_{\text{pre-irradiation}}/\kappa_{\text{post-irradiation}}$, the effects for the two nanowires are plotted in Fig. 2b over the available temperature range of 260–300 K. It is observed

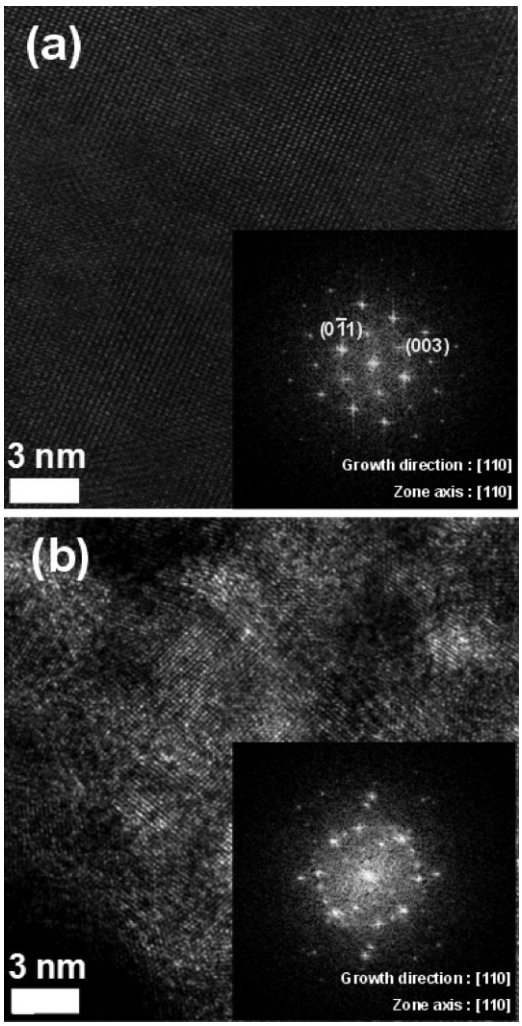

Figure 3 (a) High-resolution TEM image of a single-crystalline Bi nanowire ($d_w = 154$ nm) before proton irradiation. The inset shows a selected area electron diffraction (SAED) pattern for the Bi nanowire. The SAED pattern of the nanowire indicates that the nanowire was grown in the [110] direction with high-quality single-crystallinity. (b) A high-resolution TEM image of the Bi nanowire after proton irradiation. The SAED pattern in the inset shows that the single-crystallinity was destroyed after exposure to protons.

from Fig. 2b that the thermal conductivity change for 154 nm Bi nanowire (B) is higher than that for 112 nm Bi nanowire (A), implying that the conductivity change is proportional to deposition energy. The ratios of thermal conductivity changes between the 112 and 154 nm nanowires (A/B), the normalized deposition energy ratio, and total deposition energy ratio are also included in Fig. 2b. The relative ratio of A/B had little correlations with the total deposition energies, whereas it is in fairly well agreement with the ratio of normalized deposition energies within the considered temperature range (260–300 K). This reflects that the incident protons would have more chances to interact with the target atoms under uniform affluence in thicker nanowires.

In order to confirm any structural changes of Bi nanowires occurring through proton irradiation, high-resolution transmission electron microscopy (HR-TEM) was employed. Figure 3 shows the high-resolution TEM images of an as-grown Bi nanowire and a proton-irradiated Bi nanowire with corresponding selected area electron diffraction (SAED) patterns in the insets. The TEM image of the as-grown Bi nanowire reveals high-quality single-crystallinity with a growth direction of [110] (Fig. 3a). On the other hand, the TEM image of the proton-irradiated Bi nanowire shows a destruction of the single-crystallinity, represented by various defects such as grain boundaries, point defects, and local amorphous spots, which were most likely generated by the impingement of high-energy protons. For this reason, the SAED pattern of the proton-irradiated Bi nanowire exhibits smeared major spots, weak rings, and scattered small spots, as shown in the inset of Fig. 3b. Considering this with the thermal conductivity results discussed earlier, it seems to be plausible to conclude that the thermal transport in proton-irradiated Bi nanowires is substantially suppressed by various crystal defects induced through protons-Bi atoms interactions that may significantly reduce the phonon mean free path.

4 Conclusions In summary, the thermal conductivities of individual single-crystalline Bi nanowires, which were grown by the OFF–ON method, were measured using suspended MEMS before and after proton irradiation, respectively. The thermal conductivity substantially decreased and the crystal structure was significantly destructed after exposure to protons, indicating that thermal transport through a Bi nanowire is suppressed due to the destruction of crystal lattice by proton irradiation. From the simulation and experimental data, the decrease in thermal conductivity was more pronounced at thicker Bi nanowires, justifying that the irradiated proton particles have more chances to interact with the target atoms under uniform affluence in thicker nanowires. Our results suggest that proton irradiation plays a significant role in determining thermal transport in Bi nanowires and this effect should be brought under serious consideration for any thermoelectric applications.

Acknowledgements This work was supported by the KARI-University Partnership Program, the Pioneer Research Center Program (2010-0019313) and the Priority Research Centers Program (2009-0093823) through the National Research Foundation of Korea (NRF).

References

[1] W. Shim, J. Ham, K. I. Lee, W. Y. Jeung, M. Johnson, and W. Lee, Nano Lett. **9**, 18 (2008).
[2] K. Liu, C. L. Chien, P. C. Searson, and Y. Z. Kui, Appl. Phys. Lett. **73**, 1436 (1998).
[3] L. D. Hicks and M. S. Dresselhaus, Phys. Rev. B **47**, 12727 (1993).
[4] Y. M. Lin, X. Z. Sun, and M. S. Dresselhaus, Phys. Rev. B **62**, 4610 (2000).
[5] Y. M. Lin, S. B. Cronin, J. Y. Ying, M. S. Dresselhaus, and J. P. Heremans, Appl. Phys. Lett. **76**, 3944 (2000).
[6] M. S. Dresselhaus, Y. M. Lin, O. Rabin, and G. Dresselhaus, Microscale Therm. Eng. **7**, 207–219 (2003).
[7] A. Nikolaeva, T. E. Huber, D. Gitsu, and L. Konopko, Phys. Rev. B **77**, 035422 (2008).
[8] J. Heremans and C. M. Thrush, Phys. Rev. B **59**, 12579 (1999).
[9] Z. B. Zhang, X. Z. Sun, M. S. Dresselhaus, J. Y. Ying, and J. Heremans, Phys. Rev. B **61**, 4850 (2000).
[10] W. Shim, J. Ham, J. Kim, and W. Lee, Appl. Phys. Lett. **95**, 232107 (2009).
[11] T. W. Cornelius, M. E. Toimil-Molares, R. Neumann, and S. Karim, J. Appl. Phys. **100**, 114307 (2006).
[12] A. Boukai, K. Xu, and J. R. Heath, Adv. Mater. **18**, 864 (2006).
[13] D. S. Choi, A. A. Balandin, M. S. Leung, G. W. Stupian, N. Presser, S. W. Chung, J. R. Heath, A. Khitun, and K. L. Wang, Appl. Phys. Lett. **89**, 141503 (2006).
[14] A. Khitun, A. Balandin, K. L. Wang, and G. Chen, Physica E **8**, 13 (2000).
[15] E. P. Pokatilov, D. L. Nika, and A. A. Balandin, Phys. Rev. B **72**, 113311 (2005).
[16] J. Zou and A. Balandin, Phys. J. Appl. Phys. **89**, 2932 (2001).
[17] A. L. Moore, M. T. Pettes, F. Zhou, and L. Shi, J. Appl. Phys. **106**, 034310 (2009).
[18] J. W. Roh, K. Hippalgaonkar, J. H. Ham, R. Chen, M. Z. Li, P. Ercius, A. Majumdar, W. Kim, and W. Lee, ACS Nano **5**, 3954 (2011).
[19] M. J. Smith, J. Appl. Phys. **34**, 2879 (1963).
[20] P. Chaudhari and M. B. Bever, J. Appl. Phys. **38**, 2417 (1967).
[21] J. Ham, W. Shim, D. H. Kim, S. Lee, J. Roh, S. W. Sohn, K. H. Oh, P. W. Voorhees, and W. Lee, Nano Lett. **9**, 2867 (2009).
[22] J. W. Roh, S. Y. Jang, J. Kang, S. Lee, J.-S. Noh, W. Kim, J. Park, and W. Lee, Appl. Phys. Lett. **96**, 103101–103103 (2010).
[23] A. I. Hochbaum, R. K. Chen, R. D. Delgado, W. J. Liang, E. C. Garnett, M. Najarian, A. Majumdar, and P. D. Yang, Nature **451**, 163 (2008).
[24] D. Y. Li, Y. Y. Wu, P. Kim, L. Shi, P. D. Yang, and A. Majumdar, Appl. Phys. Lett. **83**, 2934 (2003).
[25] G. F. Knoll, Radiation Detection and Measurement (Wiley, New York, 2000).
[26] MCNPX User's Manual Version 2.4.0: Los Alamos Natl. Lab. Rep. LA-CP-02-408.

